BUTTERWORTH HEINEMANN

Polymer Vol. 36 No. 7, pp. 1331–1339, 1995

0032-3861/95/$10.00 + 0.00

polymer papers

On the structure of ultra-high molecular weight polyethylene gels

Martin Kunz
Institut für Makromolekulare Chemie, Universität Freiburg, Stefan-Meier-Strasse 31, D-79104 Freiburg, Germany

and Markus Drechsler
Institut für Biophysik und Strahlenbiologie, Universität Freiburg, Albertstrasse 23, D-79104 Freiburg, Germany

and Martin Möller*
Universität Ulm, Organische Chemie III/Makromolekulare Chemie, D-89069 Ulm, Germany
(Received 5 August 1993; revised 21 August 1994)

Gel-crystallized ultra-high molecular weight polyethylene samples have been studied by transmission electron microscopy (TEM) and differential scanning calorimetry. The microstructure of the gels was investigated by substitution of the solvent by methacrylate monomers which were subsequently cured by ultraviolet radiation at low temperature. TEM images of RuO_4-stained thin sections showed a network of lamella crystals in which the links were formed by local contacts of the crystal surfaces. Electron spectroscopic imaging yielded carbon concentration profiles across the width of isolated crystals. Annealing of the dried gels above T_α illustrated a high mobility of the polyethylene chains within the crystal above the α-transition and well below the melting point. Long lamellae became decorated by shorter and thinner crystallites which appear to be grown perpendicular on the surface of the long ones.

(Keywords: polyethylene gels; crystal structure; transmission electron microscopy)

INTRODUCTION

Thermoreversible ultra-high molecular weight polyethylene (UHMW-PE) gels can be employed as precursors for the preparation of fibres with excellent mechanical properties[1–3]. The gels are formed by cooling solutions of UHMW-PE in decaline or xylene from a temperature above the dissolution temperature of polyethylene to room temperature[4]. Many investigations have been performed on films obtained after drying of the gels[5–12]. Electron microscopy experiments on dried and freeze-dried samples showed agglomeration of interconnected single crystals[9,10]. There are only a few reports on the structure of the initially formed gel that still contains the solvent. Sawatari *et al.* performed viscosity measurements in dependence of the concentration and molecular weight and found a critical concentration for gel formation[6]. Chung and Zachariades carried out rheo-optical measurements on UHMW-PE in paraffin oil[13]. Spherulites and stacks of single crystals were observed by polarizing microscopy[14].

In the present work, we report a preparation method that allows us to investigate the gels as prepared in solution, avoiding the drying step. Transmission electron microscopy (TEM) studies on UHMW-PE gels have been performed to determine the effects of concentration, cooling condition and annealing temperature on microstructure. Differential scanning calorimetry (d.s.c.) was used to determine melting temperatures and crystallinities.

EXPERIMENTAL

Polyethylene (PE) gels were prepared from solutions of UHMW-PE (Hizex 240M, $M_w = 1.5 \times 10^6$) in decalin according to the method of Smith and Lemstra[4]. The hot solution was annealed for 4 h and cooled to room temperature. Either concentrations were varied between 0.5 and 6 wt% while crystallization conditions were kept constant or the concentration was 1.5 wt% and the cooling rate was varied. The highest cooling rate was obtained by pouring the hot solution into a Büchner funnel with a PTFE filter on the bottom, covering it immediately with cooled hexane (−70°C) and sucking the cold hexane through the gel (sample G-I). A second sample (G-II) was prepared by allowing the PE solution to cool down under ambient conditions. The lowest cooling rate of $0.7\,K\,h^{-1}$ was achieved by cooling the solution in a closed glass cylinder within a thermostat (sample G-III). A fourth sample (G-IV) was crystallized by cooling the solution slowly to 90°C, followed by annealing for 1 week at this temperature before cooling to room temperature.

* To whom correspondence should be addressed

For the TEM studies, a small part ($\sim 0.5\,cm^3$) of the gel was separated by means of a sharp knife and quickly transferred into a glass beaker filled with solvent. The remaining, bigger part was squeezed to the bottom of the glass beaker and the solvent was decanted. Drying was performed at 50°C at a pressure of ~ 2.7 kPa while the sample was placed between two parallel glass plates and put under a load of 4 kg. Dried gel films were annealed for 1 h at different temperatures up to 165°C while they were compressed between parallel plates (4.9 MPa). Afterwards, the samples were allowed to cool slowly to room temperature while they were kept under pressure.

Specimens for TEM observation were prepared by transferring a small piece of the gel into a mixture of methacrylate monomers with 0.1% benzoin as a photo-initiator (Lowicryl HM 20, Chemische Werke Lowi GmbH). The decalin was subsequently extracted several times by replacing the solvent/monomer mixture by new monomer. Special care was taken to keep the gel always covered with liquid. Samples were placed into BEEM (Bal-Tec, Walluf) capsules (polyethylene 5.2 mm diameter, Serva), and polymerization was initiated at -40°C by indirect and diffuse u.v. irradiation[15,16]. This prevented structural changes and local overheating and resulted in slow and homogeneous curing. The highly crosslinked methacrylate resin used for embedding did not show a glass transition in d.s.c. experiments.

To fix the dried and compressed films for microtomy, the samples were embedded in epoxy (Epon 812, Serva), cured for 48 h at 65°C[17] and stained with ruthenium tetroxide[18]. Staining was performed after embedding and before sectioning since the RuO_2 interfered with the u.v. polymerization and led to inhomogeneous hardening of the sample. Staining before sectioning caused additional hardening and adhesion between the embedding matrix and the PE crystals and allowed thinner sections to be obtained.

Ultra-thin sections were cut at room temperature with an Ultracut E microtome (Reichert & Jung) equipped with a diamond knife. All sections were prepared from the region in the centre of the embedded gel to ensure that images were recorded from areas where no orientation or destruction of the structure had occurred during handling of the sample. Dried embedded films were cut perpendicular to the film surface. Specimens with a thickness of 50 nm or less were selected by the silvery to colourless interference.

Electron micrographs were recorded on Scientia film (Agfa Gevaert) by means of a Zeiss EM 902 with integrated electron energy loss spectrometer and a Philips 400 electron microscope working with acceleration voltages of 80 and 100 kV, respectively. Wide-angle electron diffraction (WAED) was performed on both microscopes at camera lengths of 421 and 316 mm. Low-angle electron diffraction (LAED) was performed with the Philips 400 at a camera length of 1199 mm. Calibration was done using cross-grating replicas, thallium chloride and catalase crystals. Images of net-element distributions and concentration profiles were obtained using an IBAS image processing system (Kontron) which was directly connected to the Zeiss EM 902 via a silicon-intensified target video camera (Dage-MTI, Inc.). A detailed description of electron specific imaging as a means to record element distributions is described in the literature[19–21].

Several negatives were used for the determination of crystal thickness and more than 200 crystals were measured in each case. Special care was taken to measure only those lamellae which were obviously not inclined with respect to the viewing direction. The distance between the stained crystal surfaces gave the crystal thickness. The long period was determined from the width of a stack of parallel crystals divided by their number (accuracy of ± 0.5 nm) or from the corresponding low-angle diffraction spots. Because of the high orientation, the long period determined by low-angle diffraction gave the same results as measurements on the micrographs.

Dried gel samples of 1–2 mg weight were studied at a standard heating rate of 10 K min^{-1} using a Perkin–Elmer DSC-7 differential scanning calorimeter. When samples were annealed in the d.s.c. apparatus, they were cooled to room temperature at a cooling rate of 20 K min^{-1}. The instrument was calibrated with high purity gallium and indium standards. Transition enthalpies as determined by numerical integration of the transition peaks showed a variation of $<5\%$. The crystallinity was calculated by assuming a melting enthalpy of 293 J g^{-1} for 100% crystalline material.

RESULTS AND DISCUSSION

Embedded 'solvent'-containing gels

To study the gels by TEM, the structure had to be fixed and thin sections had to be prepared. Corresponding to techniques which have been developed to arrest the structure of biological samples consisting of water-containing 'jelly' cells[15–17,22], the xylene in the PE gel was replaced by a mixture of methacrylate monomers which could be polymerized at low temperatures, initiated by indirect and diffuse u.v. irradiation. The low viscosity and hydrophobicity of the monomer mixture allowed rapid penetration into the gel. Miscibility with the original solvent facilitated the substitution.

No swelling or shrinkage of the jelly sample could be observed during this procedure. The results obtained from electron microscopy have been reproduced with different samples and did not vary when the curing temperature and the curing rate were changed within reasonable limits. Therefore, it can be concluded that the images represent the gel structures faithfully.

Micrographs of the PE gels showed a network structure of randomly distributed chain-folded single crystals (*Figure 1*). The crystals appear as thin, bright stripes with dark borders. The dark borders are due to the preferential reaction of the folded, constrained chains in the crystal surfaces with the staining agent, i.e. RuO_4 (ref. 23).

The gel network was formed by alignment of short lamella segments with (dark) interlayers of amorphous material as the actual connection. Checking the structures carefully on a large number of micrographs, we could not observe branching points, where the lamellae themselves ramify. Therefore, the gel topology is described by bridges of isolated (or a few stacked) lamellae which are locally interconnected by adhesion of the crystal surfaces. Syneresis effects which occurred in the late stages of cooling indicate that tie molecules that remained dissolved might become strained during crystallization and act like springs which pull the lamellae together (see also *Figure 8* below).

Figure 1 Electron micrographs of a polymethacrylate embedded polyethylene gel prepared by cooling a 3 wt% solution in xylene from 135°C to room temperature: (a) network of connected single crystals, (b) high magnification of an edge-on view of a crystal–crystal junction

Isolated single crystals could be studied by means of electron spectroscopic imaging (e.s.i.), yielding the carbon concentration profile across a single crystal. The carbon distribution of the sample was monitored by means of an integrated electron energy loss spectrometer, allowing selective imaging of electrons which were inelastically scattered at the carbon K-shell. To obtain the net-element distribution, a second image with the background intensity (in front of the adsorption edge) was subtracted using an image process[19–21].

The elastic bright-field image (only elastically scattered electrons were recorded) in *Figure 2a* shows two polyethylene crystals edge-on which are linked together via the lamella surface. The carbon net-element distribution is depicted in *Figure 2b*. The crystalline parts appear as bright stripes because the intensity in this image is linearly related to the carbon concentration and the maximum carbon density is found inside the crystals. *Figure 2c* shows the intensity profiles along the bright lines in the micrographs *a* and *b*. The contrast improvement in the net-element distribution image is significant compared with the elastic bright-field image. Profile *b* represents the relative carbon concentration across the crystals. (Small peaks next to the main signal, which are particularly visible in diagram *b*, show variations in the local carbon concentration along the scan line which are caused by the presence of RuO_2 particles.) The observed gradual increase of the carbon density starting from low values at the surface of the crystal and reaching a maximum in the middle of the lamella might be explained by variations in the packing of the chain segments affected by the irregularity at the surface[24,25].

Figures 3 and *4* demonstrate some peculiarities in the shape of the isolated crystallites. It cannot be excluded that at least some of the features in *Figures 3* and *4* were formed after crystallization, e.g. by shrinkage of the gel. Typically, the crystals formed curved, dome-like structures (*Figure 3a*). The structures appear thicker than in reality because the picture was taken in underfocus in order to increase the contrast. Further, only lamellae which are oriented at an angle close to 90° with respect to the plane of the section are depicted sharply. *Figure 3b* shows a slice through such a dome normal to its azimuth. In this picture, the stained lamella surfaces are inclined and are shown as a dark smeared ring.

Figure 3c gives an example of a ridged structure. Ridged crystals have been reported in investigations on single crystals[26], where electron diffraction experiments had demonstrated that the chains were inclined at an angle of 58° relative to the surface[27]. The zigzag structures which we have found in the case of the PE gels form an angle of ~120°, which corresponds to an inclination angle of the chains of roughly 60°. Thus the results found for the embedded gels match the inclination angle reported on single crystals, and the formation of the corrugations is consistent with crystal twinning.

Rather peculiar structures were observed when thicker sections (~200–300 nm) were investigated. *Figure 4* shows a crystal which is twisted and forms a helix. Only the edge-on views, where the lamella surface is oriented normal to the viewing direction, show the parallel lines of the stained surfaces, whereas the other parts appear not sharp due to the inclination. Twisted PE crystals have been observed before[28] and explained by the difference in stress of the two crystal surfaces, which arises from differences in the congestion of folds[29].

Diffraction experiments attempted to get more detailed information on the chain orientation and crystal structure of the ridged and twisted crystals failed since the amount of crystalline material in the selected area was too small. Also, d.s.c. experiments to detect the crystallinity of the wet gels were not reproducible because of the small PE fraction and because of the pressure build-up due to inevitable solvent evaporation.

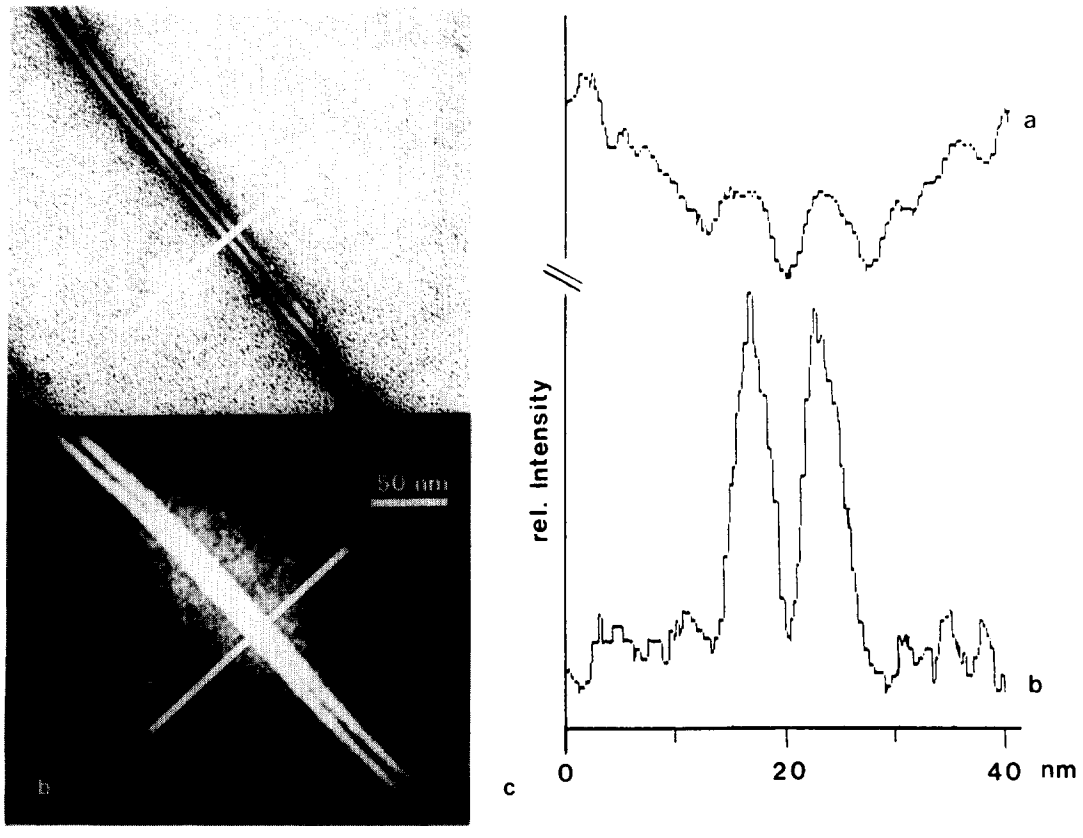

Figure 2 Electron spectroscopic imaging (E.S.I.) of a thin section of an embedded polyethylene crystal: (a) elastic bright-field image; (b) carbon net-element distribution; (c) diagrams giving the intensity profiles along the bright lines in *a* and *b*

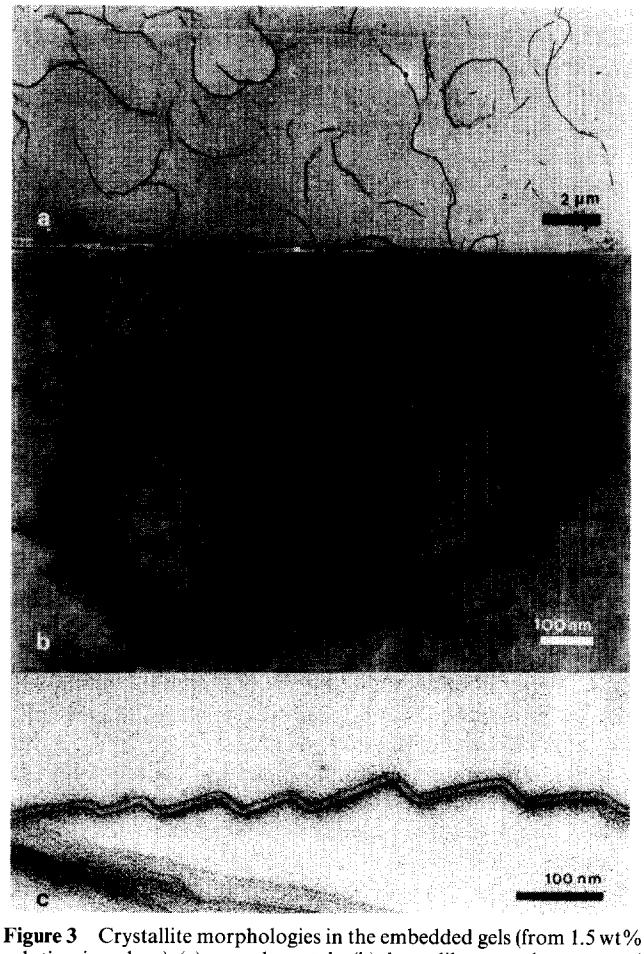

Figure 3 Crystallite morphologies in the embedded gels (from 1.5 wt% solution in xylene): (a) curved crystals, (b) dome-like crystal cut normal to its central axis; (c) edge-on view of a ridged crystal

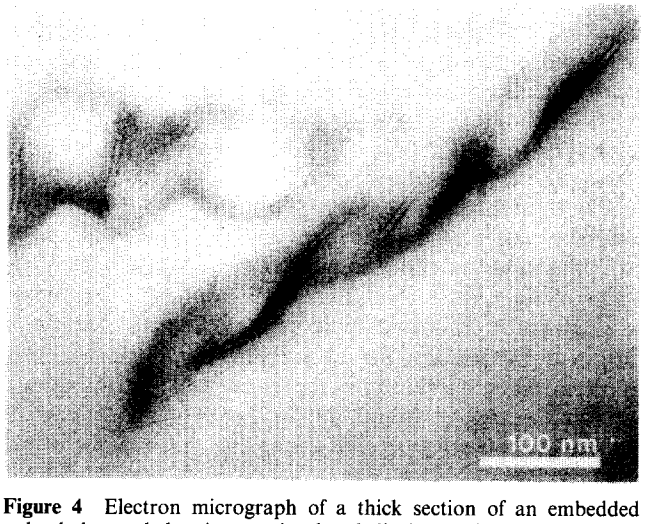

Figure 4 Electron micrograph of a thick section of an embedded polyethylene gel showing a twisted or helical crystal

Dependence of gel structure on preparation conditions

A series of samples with 1.5% polymer content was crystallized at different cooling rates to investigate the dependence of structural changes on the crystallization rate. Sample G-I was quenched to −70°C, sample G-II was cooled at ambient conditions, G-III was cooled at a rate of 0.7 K h^{-1} and G-IV was crystallized isothermally at 90°C. TEM images of the embedded gels showed short and thin crystals for sample G-I, whereas the lamellae in samples G-II and G-III exhibited increased thickness and a width reaching several μm without any visible defect.

Upon evaporation of the solvent, the sheet-like crystals oriented themselves parallel to each other and formed

stacks of lamellae. Removing half the solvent resulted in a structure where the network was not formed from single lamellae but from bundles or stacks of lamellae (*Figure 5*). Totally dried gels formed white plates whereby the white appearance is due to voids and can be removed by pressing. Compression with 4.9 MPa at 50°C did not affect the crystallinity and the melting point.

Electron micrographs of the finally dried gel film showed stacked lamellae oriented parallel to the film surface (*Figure 6*). The insert at the left corner of *Figure 6* depicts the wide-angle diffraction pattern. The (002) reflection on the meridian demonstrates that the chain axis is mainly oriented normal to the lamella surface. From the low-angle electron diffraction pattern in the right corner (arced meridional reflection, first and second order) the long period was calculated to be 7.1 nm, which coincides with the value obtained by measurements on the micrographs. Comparison with the lamella thickness observed for the wet gels shows that no significant variation occurred upon drying and compression.

Morphological and thermal data on the dried gels are compared in *Table 1*. The crystal thickness data are mean values from electron micrographs of the dry gels. Long periods were obtained from low-angle electron diffraction patterns. As to be expected, crystallinity, crystal thickness and long period increased with decreasing cooling rate[30,31].

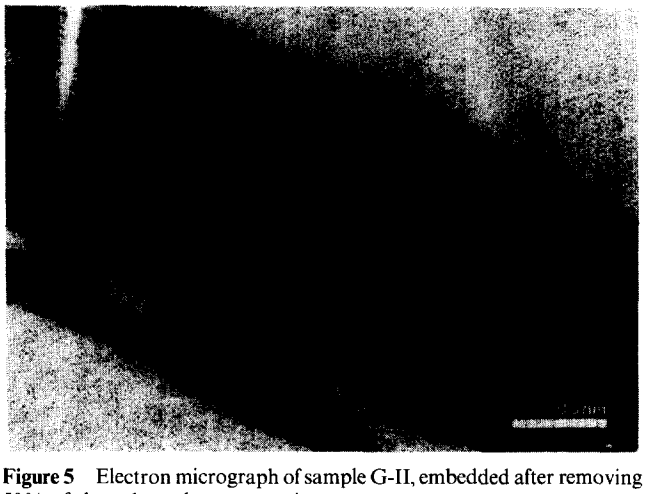

Figure 5 Electron micrograph of sample G-II, embedded after removing 50% of the solvent by evaporation

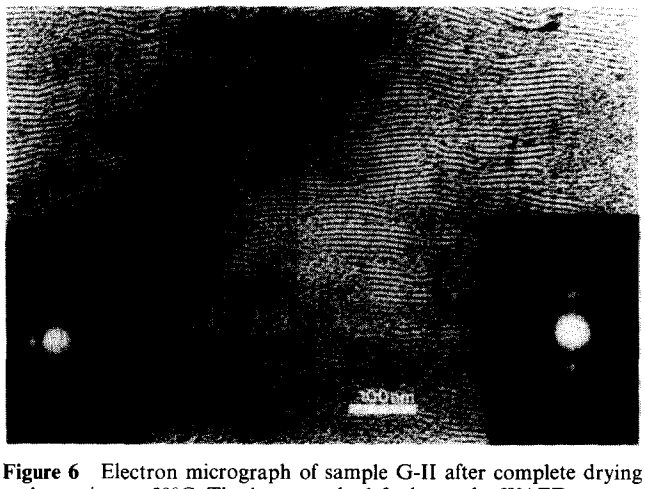

Figure 6 Electron micrograph of sample G-II after complete drying and pressing at 50°C. The inset on the left shows the WAED pattern and inset on the right the LAED pattern of the same sample area

Table 1 UHMW-PE gels prepared from 1.5% xylene solutions under different cooling conditions

Sample	T_{mo}[a] (°C)	T_{mp}[b] (°C)	w_c[c] (%)	d[d] (nm)	l[e] (nm)	$l-d$[f] (nm)
G-I	133	137	70	4.1	6.4	2.3
G-II	126	136	74	4.5	6.9	2.4
G-III	126	135	80	5.1	7.4	2.3
G-IV	124	133	79	6.5	8.7	2.2

[a] Onset of melting peak
[b] Melting point
[c] Crystallinity
[d] Crystal thickness of dry gel
[e] Long period
[f] Thickness of amorphous region

Table 2 Annealed UHMW-PE gel films prepared from 1.5% xylene solutions

Sample	T_a[a] (°C)	T_{mo}[b] (°C)	T_{mp}[c] (°C)	w_c[d] (%)	d[e] (nm)	l[f] (nm)	$l-d$[g] (nm)
G20	20	127	132	74	4.7	7.1	2.4
G50	50	127	133	74	4.7	7.1	2.4
G90	90	127	136	75	5.7	8.5	2.8
G100	100	128	136	76	6.3	10.4	4.1
G110	110	128	137	76	7.5	13.1	5.6
G120	120	134	140(125)	60	8–13	20[h]	7–10[h]
G125	125	129	138(130)	56	10–20	–	–
G165	165	123	132	48	8–15	–	–

[a] Annealing temperature
[b] Onset of melting peak
[c] Melting point
[d] Crystallinity
[e] Crystal thickness
[f] Long period from electron diffraction
[g] Thickness of amorphous region
[h] Value only estimated from micrographs

A crystallinity of 80% for the dried gels (by d.s.c.) appears to be the maximum value achievable in this system, which is in good agreement with data of Smith[32]. The long period as well as the lamella thickness of the gel-crystallized samples were significantly smaller than the values obtained for polyethylene of smaller molecular weight crystallized from solution at comparable temperatures. Even for the lowest crystallization temperature, a long period of about 10 nm has been reported in the literature[33], whereas in our case the highest value has been found to be 8.7 nm for the isothermally crystallized sample G-IV.

Annealing of embedded gels

As the interface to the matrix can serve as an internal reference line, annealing experiments on the embedded gels are helpful in visualizing crystal reconstruction. When the embedded samples were annealed for 96 h above the α-transition either at 100°C or close to the melting transition at 123°C, the long lamellae broke up into smaller crystallites with rounded edges (*Figure 7a*). In the case of totally isolated lamellae, the stiff resin matrix restricted lamellae thickening efficiently. When two lamellae were in direct contact with each other, lamella thickening and splitting or twinning was observed

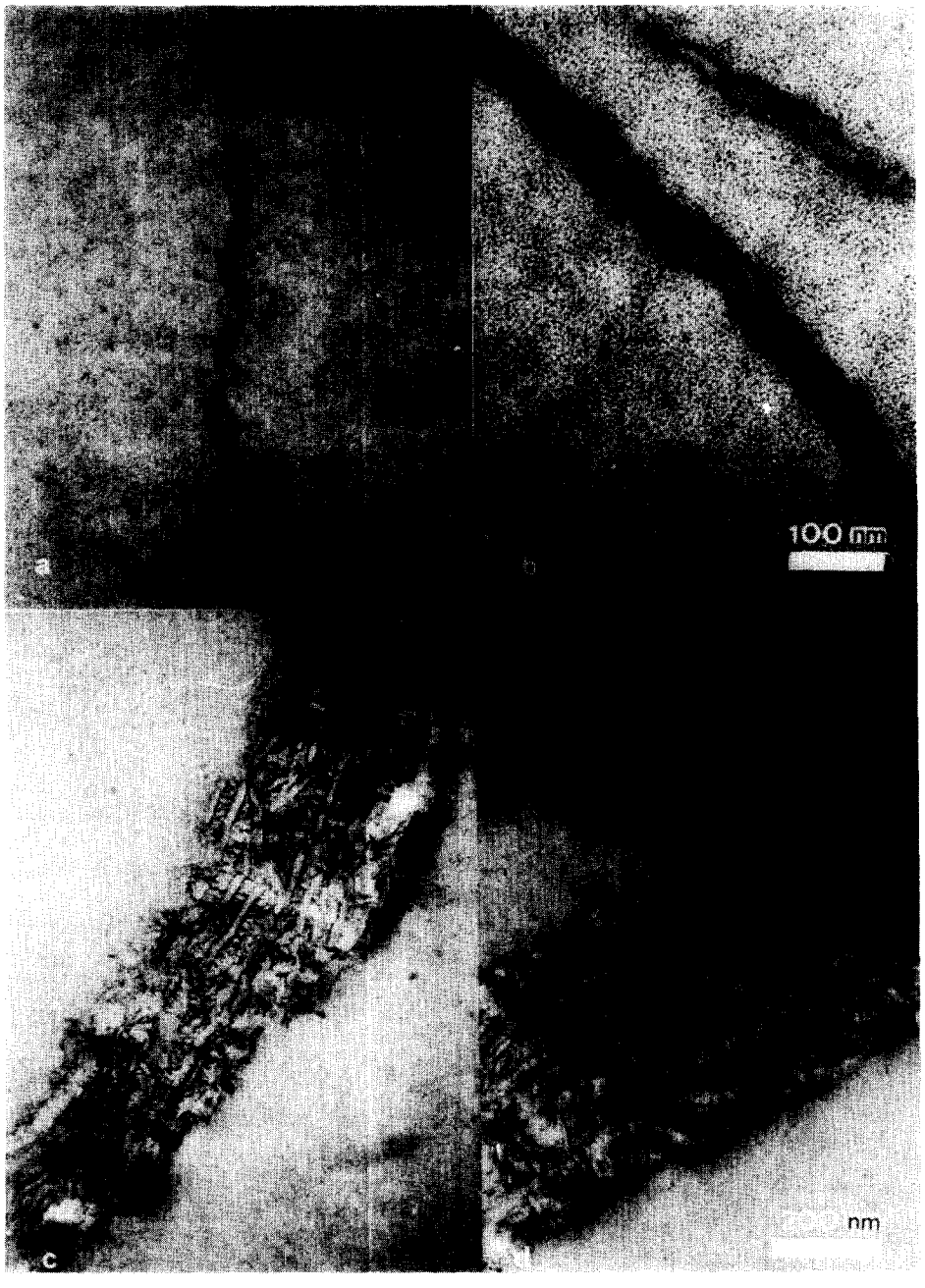

Figure 7 Electron micrographs of embedded gels which were prepared from 1.5% xylene solution and annealed for 96 h at: (a) 100°C; (b) 110°C, (c) 123°C; and (d) 1 h at 150°C. Magnifications of *a* and *b* and of *c* and *d* are identical

at 100°C (*Figure 7b*) while at 123°C, stacks of lamellae formed a peculiar morphology which is depicted in *Figure 7c*. Some of the lamellae remained parallel to the PE–resin interface but were increased in thickness from ~6 to 12 nm, whereas other crystals had a decreased width and were rotated by 90°. A similar effect was also observed for the dried gels and is shown in *Figure 10*.

Increasing the temperature to 150°C and subsequent recrystallization altered the structure completely. The melt trapped in the unyielding matrix could not rebuild the original structure. Arbitrarily arranged crystals of decreased and varying size were observed with rounded edges (*Figure 7d*).

Annealing of dried gels

Results of d.s.c. measurements and electron microscopy on the annealed dried films are summarized in *Table 2*. Numbers in the sample code indicate the temperature at which the sample was annealed, e.g. G100 was annealed at 100°C. The annealing temperature was set to 20°C for samples which were always kept at room temperature.

The small increase of crystallinity observed for annealing temperatures up to ~110°C is within the experimental error of about 3.5% ($10\,J\,g^{-1}$). The decrease in crystallinity and the observation of a second endotherm upon annealing at higher temperature are consistent with partial melting of the smallest crystals accompanied by perfection and growth of the bigger crystals[34]. Increasing the annealing temperature above the melting point of the gel films resulted in recrystallization from the melt and reduced the degree of crystallinity to 47.8%.

The micrographs in *Figure 8* show that the order in the annealed gel films remained more or less the same up to 110°C. Significant disordering of lamellae started

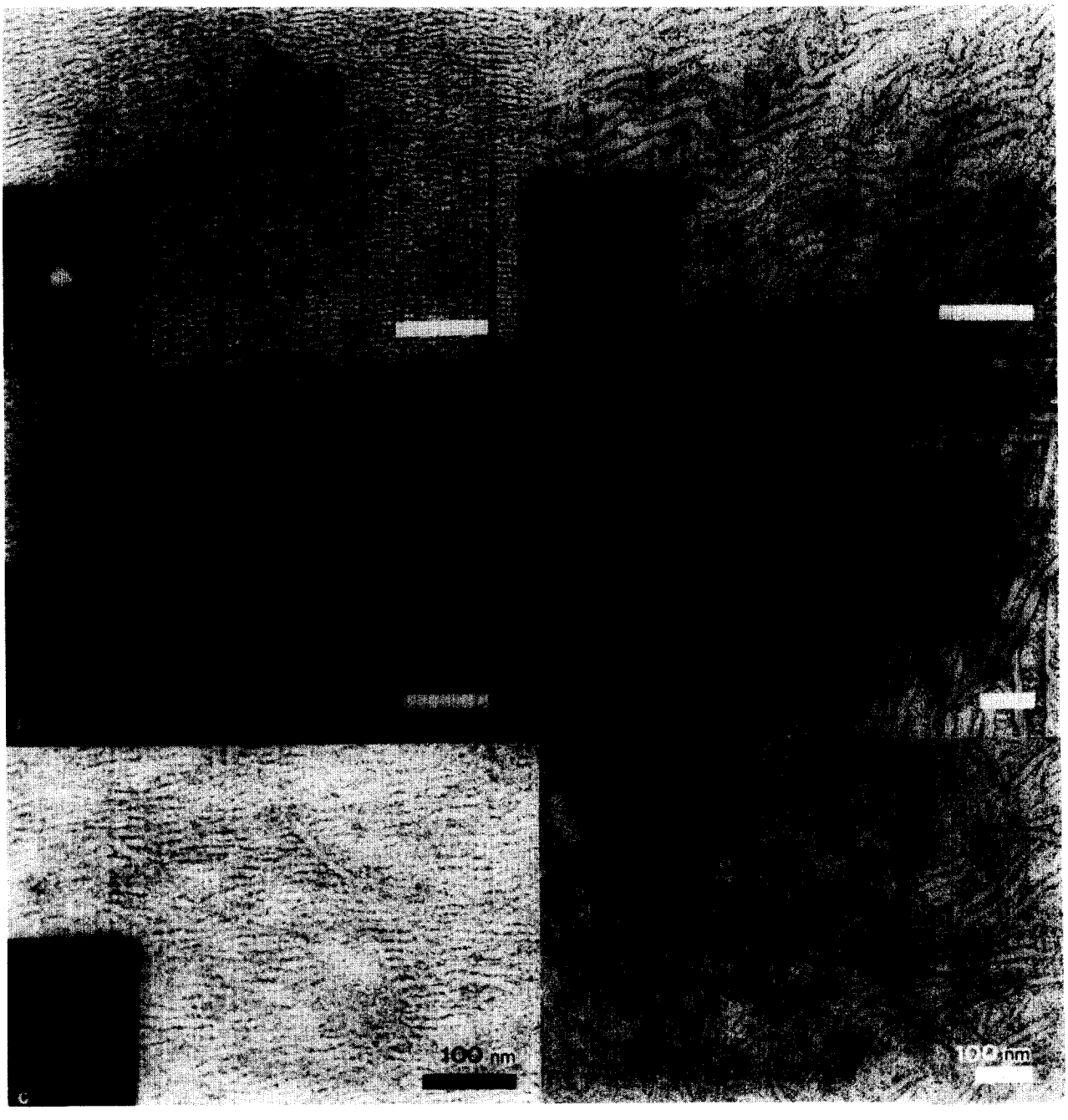

Figure 8 Electron micrographs, LAED and WAED patterns of dry gel films annealed at different temperatures: (a) G90; (b) G100; (c) G110; (d) G120; (e) G125; (f) G165. Notice the change in magnification from *d* to *e*

above 120°C (*Figure 8d*). The stained interface became thicker while the surface of the lamellae became more and more irregular. Clear evidence was given for lamella thickening whereby the crystals seem to merge or grow into each other. While an increase in the long period and the lamella thickness has been reported before[5,8,25,35–38], our results give clear evidence that the long period grew faster than the crystal thickness (*Table 2*, *Figure 9*). Hence, the increase in long period is not only due to growth of the crystal thickness, but is also caused by broadening of the amorphous interface.

As already discussed for the annealed embedded gels, micrographs of the gel films G120 and G125 also showed thick lamellae which were surrounded by thinner crystallites oriented perpendicular to their surface. This is demonstrated in *Figure 10* for the sample G120. Horizontally arranged lamellae with a thickness of 8–10 nm appear to be embedded in a matrix of vertically directed lamellae with a thickness of 6–10 nm. Wide-angle electron diffraction experiments proved the existence of two sets of crystallite orientations (inset of *Figure 10*). Both the (1 1 0) as well as the (2 0 0) reflections near the central beam form four-point patterns and the connecting lines of the corresponding spots are perpendicular to each other.

In the case of sample G125, the thicknesses of the transversely oriented crystallites were 10 and ~20 nm, respectively. Due to the lower degree of orientation, wide-angle electron diffraction resulted in extended arcs (inset of *Figure 8e*) and clear identification of the chain directions was not possible. It may be assumed, however,

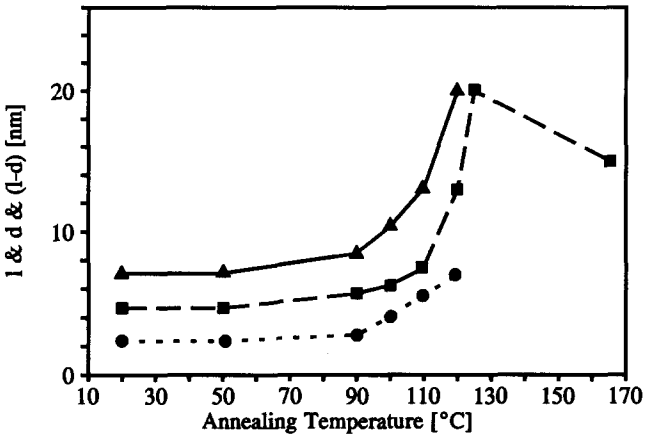

Figure 9 Variation of crystal thickness d (--■--), long period l (—▲—) and interface thickness l–d (-- ● --) with annealing temperature

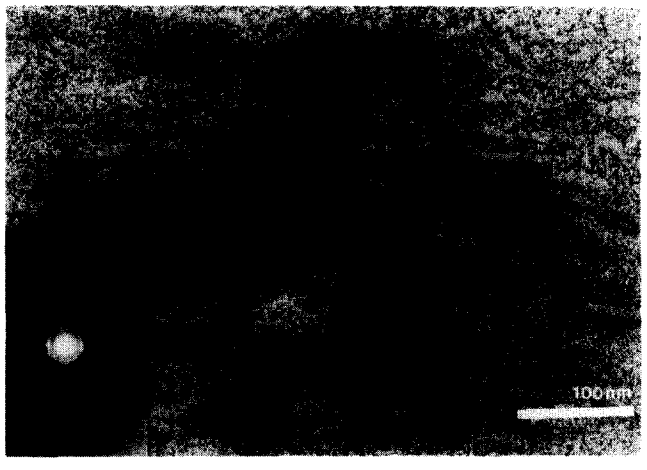

Figure 10 Electron micrograph of an oriented area of sample G120 with the corresponding WAED pattern showing long lamellae in the horizontal direction decorated by vertically arranged smaller ones

that in this case also the chains are directed perpendicular within the transversely oriented crystallites. The observation of two types of crystallites is consistent with the calorimetric data in *Table 2* showing two melting endotherms.

After bringing the sample to 165°C, the crystal thickness dropped to 8–15 nm which is consistent with the lower melting point compared with that of G125. At the same time a completely isotropic distribution of the crystallite orientation was formed (*Figure 8d*), as to be expected after recrystallization from the melt[11,39].

CONCLUSIONS

Substitution of the solvent by a monomer mixture and subsequent u.v.-curing allowed us to study the morphology of crystalline polymer gels. Thus, it was possible to observe structural details complementary to the results which can be obtained by scanning electron microscopy techniques[9,40]. Further, it has been demonstrated that electron spectroscopic imaging can give new information on the structure and local elemental composition of polymers with high resolution.

The electron micrographs of the 'solvent'-containing gels depicted a network which was formed from bridges of isolated (or a few stacked) lamellae locally linked by adhesion of the crystal surfaces. Dissolved tie molecules might play an important role in determining the observed topology as they become strained during crystallization and act like springs which pull the lamellae together.

In the embedded gels as well as in the dried films, the thickness of the UHMW-PE lamellae was significantly smaller than that observed when polyethylene of lower molecular weight is crystallized from solution[33]. An explanation for this observation may be that the longer relaxation time of the UHMW-PE molecules influences the crystallization, e.g. by lowering the chain alignment probability[41,42]. On the other hand, long periods reported in the literature have been measured by small-angle X-ray scattering (SAXS) and there is a difference in the average values obtained by TEM and SAXS due to sample orientation.

Different and sometimes concurrent processes have been observed by annealing experiments in combination with TEM investigations: (i) lamella thickening, d; (ii) thickening of the amorphous layer; and (iii) premelting.

Upon annealing below 110°C, a considerable mobility of the chain segments inside the crystallites was indicated by the observation that the crystallites not only thickened but grew virtually into each other. As the disordered segments in the interface between the crystals have to be incorporated into the crystals, the chains must be able to move through the thickening crystal as has been demonstrated by ^{2}H n.m.r.[43].

An increase of the stained 'amorphous' layer upon annealing has also been reported for very thin melt-spun polyethylene films[44]. A raised degree of crystallinity in combination with an increase in the thickness of the 'amorphous' interlayer might be explained by a rather high degree of ordering in the lamellae surfaces. Also, higher melting enthalpies can be achieved by perfection of the crystallites.

A peculiar reorganization occurred when embedded gels as well as dried films were annealed at or slightly above 120°C. Thickened long lamellae, which were oriented as before annealing, became decorated by shorter and thinner crystallites which appeared to be grown perpendicular on the surface of the long ones. It appears that nucleation of the thinner crystals is stimulated by the thicker ones. If the formation of the structure is due to epitaxy or transcrystallization, it would indicate that the surface of the thickened crystals can induce oriented crystallization and therefore should consist of highly ordered folds.

ACKNOWLEDGEMENT

Financial support was granted by the Deutsche Forschungsgemeinschaft, Sonderforschungsbereich 60. Teilprojekt A-1/F-5.

REFERENCES

1 Lemstra, P. J. and Kirschbaum, R. *Polymer* 1985, **26**, 1372
2 Barham, P. J. and Keller, A. *J. Mater. Sci.* 1985, **20**, 2281
3 Kirschbaum, R. and van Dingenen, J. L. J. in 'Integration of Fundamental Polymer Science and Technology III' (Eds L. A. Kleintjens and P. J. Lemstra), Elsevier Applied Science, London, 1989, p. 178
4 Smith, P. and Lemstra, P. J. *Makromol. Chem.* 1979, **180**, 2983

5 Matsuo, M., Sawatari, C., Iida, M. and Yoneda, M. *Polym. J.* 1985, **17**, 1197
6 Sawatari, C., Okumura, T. and Matsuo, M. *Polym. J.* 1986, **18**, 741
7 Lemstra, P. J., van Aerle, N. A. J. M. and Bastiansen, C. W. M. *Polym. J.* 1987, **19**, 85
8 Kyu, T., Futjita, K., Cho, M. H., Kikutani, T. and Lin, J.-S. *Macromolecules* 1989, **22**, 2238
9 Smith, P., Lemstra, P. J., Pijper, J. P. L. and Kiel, A. M. *Colloid Polym. Sci.* 1981, **259**, 1070
10 Barham, P. J., Hill, M. J. and Keller, A., *Colloid Polym. Sci.* 1980, **258**, 899
11 Bastiansen, C. W. M., Froehling, P., Pijpers, A. J. and Lemstra, P. J. in 'Integration of Fundamental Polymer Technology I' (Eds L. A. Kleintjens and P. J. Lemstra), Elsevier Applied Science, London, 1987, p. 508
12 Roy, S. K., Kyu, T. and John Manley, R. St. *Macromolecules* 1988, **21**, 1741
13 Chung, B. and Zachariades, A. in 'Reversible Polymeric Gels and Related Systems' (Ed. P. S. Russo), ACS Symp. Ser. 350, American Chemical Society, Washington, DC, 1986, Ch. 2, p. 22
14 Zachariades, A. *J. Appl. Polym. Sci.* 1986, **32**, 4272
15 Carlemalm, E., Gravito, R. M. and Villiger, W. *J. Microsc.* 1982, **126**, 123
16 Drechsler, M. *Thesis*, Universität Freiburg, 1990
17 Luft, J. H. *J. Biophys. Biochem. Cytol.* 1961, **9**, 409
18 Montezinos, D., Wells, G. B. and Burns, J. L. *J. Polym. Sci., Polym. Lett. Edn* 1985, **23**, 421
19 Kunz, M., Möller, M., Heinrich, U.-R. and Cantow, H.-J. *Makromol. Chem, Makromol. Symp.* 1989, **23**, 57
20 Kunz, M., Möller, M. and Cantow, H.-J. *Makromol. Chem., Rapid Commun.* 1987, **8**, 401
21 Ottensmeyer, F. P. and Andrew, J. W. *Ultrastruct. Res.* 1980, **72**, 336
22 Sawyer, L. C. and Grubb, D. T. 'Polymer Microscopy', Chapman and Hall Ltd, London, 1987
23 Kunz, M., Möller, M., Heinrich, U.-R. and Cantow, H.-J. *Makromol. Chem., Makromol. Symp.* 1988, **20/21**, 147
24 Möller, M., Waldron, R. F., Drotloff, H. and Kögler, G. in 'Integration of Fundamental Polymer Science and Technology II' (Eds L. A. Kleintjens and P. J. Lemstra), Elsevier Applied Science, London, 1988, pp. 334–341
25 Tadokoro, H. 'Structure of Crystalline Polymers', Wiley, New York, 1979
26 Bassett, D. C. in 'Principles of Polymer Morphology', Cambridge University Press, New York, 1981
27 Geil, P. H. 'Polymer Single Crystals', Interscience Publishers, New York, 1963, p. 132
28 Keith, H. D., Padden Jr, F. J., Lotz, B. and Wittmann, J. C. *Macromolecules* 1989, **22**, 2230
29 Keith, H. D. and Padden Jr, F. J. *Polymer* 1984, **25**, 28
30 Hamada, F., Wunderlich, B., Sumida, T., Hayashi, S. and Nakajima, A. *J. Phys. Chem.* 1968, **72**, 178
31 Wunderlich, B. in 'Macromolecular Physics', Vol. III, Academic Press, New York, 1980, Ch. 9.3.1
32 Smith, P. *Macromolecules* 1983, **16**, 1802
33 Wunderlich, B. in 'Macromolecular Physics', Vol. I, Academic Press, New York, 1980, Ch. 3.2.2.2
34 Sadler, D. M. and Spells, S. J. *Macromolecules* 1989, **22**, 3941
35 Peterlin, A. *J. Polym. Sci.* 1965, **C-9**, 61
36 Statton, O. W. and Geil, P. H. *J. Appl. Polym. Sci.* 1970, **3**, 357
37 Snyder, R. G., Scherer, J. R., Reneker, D. H. and Colson, J. P. *Polymer* 1982, **23**, 1286
38 Matsuo, M. and John Manley, R. St. *Macromolecules* 1983, **16**, 1500
39 Cembrola, R. J. and Stein, R. S. *J. Polym. Sci., Polym. Phys. Edn* 1980, **18**, 1065
40 Bush, P. J., Pradhan, D. and Ehrlich, P. *Macromolecules* 1991, **24**, 1439
41 Point, J. J. *Macromolecules* 1979, **12**, 770
42 Sadler, D. M. *Nature* 1987, **326**, 174
43 Schmidt-Rohr, K. and Spiess, H. W. *Macromolecules* 1991, **24**, 5288
44 Petermann, J. and Gleiter, H. *J. Polym. Sci., Polym. Phys. Edn* 1976, **14**, 555